Orientation Behavior in a Comblike Polysilane Having Long Alkyl Side Chains

A. Kaito,* T. Yatabe, S. Ohnishi, N. Tanigaki, and K. Yase

National Institute of Materials and Chemical Research, 1-1 Higashi, Tshukuba, Ibaraki 305-8565 Japan

Received March 12, 1998; Revised Manuscript Received March 15, 1999

ABSTRACT: The orientation behavior of poly(methyloctadecylsilylene) (PMOdS), a comblike polysilane having long alkyl side chains, was studied by the measurements of polarized ultraviolet (UV) and polarized Fourier transform infrared (FTIR) spectra. The oriented films were prepared by drawing on supporting polymer substrates, mechanical deposition, and crystallization on highly oriented polymer substrates. The main chains of PMOdS are oriented parallel to the drawing direction in the film drawn on polypropylene (PP) films and in the mechanically deposited film. Stretching PMOdS on polyethylene (PE) films however induces side-chain orientation along the drawing direction. The orientation behavior of PMOdS on the polymer substrates is discussed in relation to the surface morphology of the PP and PE substrates. When PMOdS is crystallized on highly oriented poly(dimethylsilylene) and poly(tetrafluoroethylene) films, the side chains tend to align in the orientation direction of the substrate polymer. Thus, the side-chain orientation competes with the main-chain orientation, depending upon the processing technique used. It is also shown that the silicon chains of PMOdS consist of various conformations and that the extended conformation orients more highly to the mechanical direction than the disordered conformation. The result of the polarized fluorescence measurement suggests that the electronic energy is transferred from the disordered conformation to the extended conformation with higher trans content.

Introduction

Polysilanes have received considerable attention of researchers because of their unique electric and optical properties,[1−6] such as electron conductivity, photoconductivity, thermochromism, photoresists, and electroluminescence. As the electronic properties originate from the delocalization of σ-electrons along the main chain, most of the properties are anisotropic with respect to the silicon chain axis. Therefore, the control of molecular orientation is an important subject not only in understanding the fundamental properties of the polymer but also in utilizing the electronic properties of polysilanes.

The oriented films of polysilanes were prepared by various processing techniques, such as hot drawing,[7−10] the Langmuir−Blodgett method,[11−14] vacuum deposition,[15−17] mechanical deposition,[18−24] and crystallization on highly oriented polymer substrates.[19,24−31] Hot drawing is one of the most fundamental methods for the processing of uniaxially oriented polymer films. It is however difficult to prepare the free-standing films of highly oriented polysilane by hot drawing, because polysilane films are generally brittle and are easily fractured at only a small strain. It is in the only reported study on this subject that the free-standing films of poly(methylethylsilylene) with high molecular weight ($M_w = 1.7 \times 10^6$) were successfully stretched to a draw ratio higher than 10.[7] To overcome the brittleness of the polysilane films, hot drawing of polysilane has been carried out in the blend films[8,9] or on the supporting polymer substrates.[10] Poly(dialkylsilanes) could be highly oriented by blending in the gel films of ultrahigh molecular weight polyethylene and by subsequent ultradrawing.[8,9] The oriented thin films of poly(dimethylsilylene) (PDMS) were obtained by casting a film of PDMS on the polymer substrate film from boiling α-chloronaphthalene solution and by subsequent drawing together with the supporting film.[10]

On the other hand, it was reported that highly oriented thin films were transferred onto the substrate surface during the friction of polymers such as polyethylene (PE) and poly(tetrafluoroethylene) (PTFE).[18] Wittmann and co-workers have recently proposed the mechanical deposition method, in which ultrathin oriented films are mechanically deposited onto the substrate by rubbing the polymer disk against the smooth substrate.[19−21] They have also reported that the mechanically deposited PTFE film is able to orient other materials which are cast or synthesized on the substrate.[19,25−27] We have applied the mechanical deposition method to prepare the highly oriented films of PDMS, which is difficult to dissolve in most organic solvents, except for α-chloronaphthalene, and does not melt before decomposition.[22−24] The oriented films of various poly(dialkylsilanes) have been prepared by casting polysilanes from solution on the highly oriented ultrathin films of PTFE and PDMS which are prepared by the mechanical deposition method.[24,28−31]

Besides molecular orientation, the molecular organization in the ultrathin films is of great importance in the properties of polysilane films. This subject has been extensively studied on the spin-cast films of poly(di-*n*-hexylsilylene) (PDHS) using UV absorption, fluorescence, and IR spectroscopy.[32−35] The relative amount of extended all-trans conformation decreases with decreasing thickness of the film, resulting in drastic changes in the UV and fluorescence spectra. The rate of crystallization and the degree of crystallinity are markedly reduced by the geometrical constraint of the ultrathin films.

Polysilanes generally contain alkyl and aryl substituents, which sometimes dominate the structure and properties of polysilanes. The side chains are expected to play an important role in controlling the orientation of polysilanes. Of particular interest is the orientation

10.1021/ma980390y CCC: $18.00
Published on Web 08/07/1999

behavior of polysilanes bearing long alkyl side chains, because the long side chains tend to orient to the mechanical direction as well as the main chains.

In this work, we prepared the oriented films of poly(methyloctadecylsilylene) (PMOdS) having long alkyl side chains, by drawing on the supporting polymer substrates, mechanical deposition, and crystallization on oriented polymer substrates. The effect of side chains on the orientation behavior was discussed for each processing method.

Experimental Section

Materials. PMOdS was synthesized by the Wurtz coupling reaction. Dichloromethyloctadecylsilane was added to molten sodium in refluxing toluene. The reaction was carried out for 20 h at 111 °C. Pouring the solution into methanol solidified the white powder, after the reaction mixture was filtrated and washed with water. Molecular weight distribution was measured using gel permeation chromatography (GPC) equipment calibrated with polystyrene standards. A bimodal molecular weight distribution was exhibited on the GPC curve of the polymer product, which was separated into two fractions with different molecular weights by repeated fractional precipitation from hexane with 2-propanol. The higher molecular weight fraction with $M_w = 400\,000$ was used for the experiment.

PMOdS films are drawn using PE, polypropylene (PP), and poly(vinyl alcohol) (PVA) as supporting films. PMOdS films were cast from hexane solution on the supporting polymer films, and the PMOdS films were co-oriented with the supporting films by stretching them at 70−140 °C.

The mechanical deposition of PMOdS was carried out using the apparatus shown in ref 24. A thick PMOdS film cast on a PE block was pressed on the surface of quartz substrate heated at 40 °C, and the thin oriented layer was transferred onto the quartz substrate by sliding the PMOdS film at a pressure of 0.3 MPa and at a velocity of 0.3 m/min.

PMOdS was also oriented by epitaxial crystallization on the highly oriented PDMS and PTFE films, which were prepared by the mechanical deposition method. The powder of PDMS, which is commercially available from Nippon Soda Co., was compressed into a disk at about 235 MPa under vacuum. The PDMS disk was slid onto a quartz substrate at a velocity of 1 m/min and a pressure of 1 MPa. The temperature of the substrate was controlled at 210 °C during deposition. The mechanical deposition of PTFE films was carried out by sliding the bulk piece of PTFE on the substrate, whose temperature was controlled at 200 °C, at a velocity of 0.3 m/min and a pressure of 0.4 MPa. The PMOdS films were spin-cast from hexane solution onto the highly oriented PDMS and PTFE films. PMOdS was epitaxially crystallized on the oriented polymer substrates.

Characterization. Thermal properties of PMOdS were investigated with a differential scanning calorimetry (DSC) using a Perkin-Elmer DSC 7 calorimeter calibrated with a standard melting temperature of Indium. The wide-angle X-ray diffraction profile was measured with the reflection method using Ni-filtered Cu Kα radiation (40 kV, 200 mA) generated by a Rota-Flex RU-300 (Rigaku-denki Co. Ltd.) X-ray diffractometer.

The polarized UV spectra were measured with a Shimadzu MPS-2000 spectrophotometer and a Glan-Thompson polarizing prism. The polarized Fourier transform infrared (FTIR) spectra were measured with a Biorad FTS-60*A*/896 FTIR spectrophotometer and a wire-grid polarizer.

The polarized fluorescence spectra were measured at an excitation wavelength of 310 nm with a fluorescence spectrophotometer, FP777 (Japan Spectroscopic Co., Ltd.), equipped with two Glan-Thompson polarizing prisms. The optical system for the polarized fluorescence measurements is shown in Figure 1, in which the *Z* and *X* axes correspond to the draw direction (DD) and the axis perpendicular to DD, respectively.

The fluorescence intensity, I_{ij}, ($i, j = X, Y, Z$) represents the intensity of a component of polarized fluorescence, which is measured with setting excitation polarization to the *i*-axis and emission polarization to the *j*-axis. The excitation beam was incident at a 25° angle from the normal of the film plane, and the fluorescence was detected at a 45° angle from the excitation beam. The polarization for the fluorescence light beam was set normal to the optical base, whereas the polarization for the excitation beam was rotated. When the draw direction, *Z*-axis, is perpendicular to the optical base (Figure 1a), the polarized fluorescence spectra, I_{xz} and I_{zz}, are measured. From the optical system shown in Figure 1b, the polarized fluorescence spectra, I_{xx} and I_{zx}, are obtained. Four components of polarized fluorescence, I_{zz}, I_{zx}, I_{xz}, and I_{xx}, can be detected by rotating the polarizer for the excitation beam and the sample direction. The polarization characteristics of the excitation spectrometer were corrected with a measured intensity of the polarized fluorescence of the isotropic sample according to the procedure shown in the appendix of ref 36.

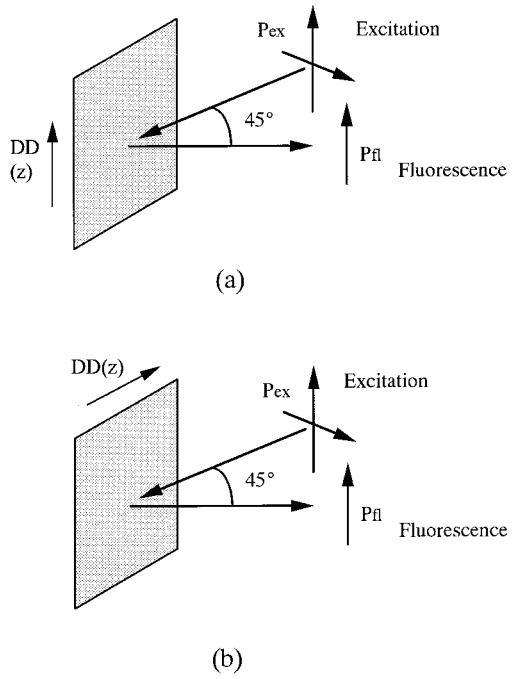

Figure 1. Optical arrangement for the polarized fluorescence measurements.

The surface morphology of the stretched films was examined with scanning electron microscopy (SEM) and scanning force microscopy (SFM). SEM images were obtained with a TOPCON DS-720 scanning electron microscope, after the sample surface was coated with a plasma-polymerized OsO_4 film. SFM was examined with a Nanoscope IIIa (Digital Instruments, Inc.) equipped with a 200 μm long cantilever with a triangular silicon nitride tip. The nominal spring constant of the cantilever is 0.12 N/m. The images (512 × 512 pixels) were taken with a 150 μm × 150 μm scanner (J-scanner) with "height mode" and "friction mode". The height mode, which keeps the force constant, was employed to estimate the surface roughness; meanwhile, the friction mode was used to observe the detailed structure of the surfaces. The typical force acting on the surfaces during imaging was 1−2 nN.

Results and Discussion

Structure and Thermal Properties of PMOdS. PMOdS shows an endothermic peak at 51.25 °C on the DSC curve with associated enthalpy change of 81 J/g. No birefringent structure was observed in the polarized optical microscopy above the phase transition temperature. Therefore, the endothermic peak was ascribed to the first-order transition from crystal to isotropic melt. The order of crystal structure in the low-temperature phase was examined by wide-angle X-ray diffraction. An

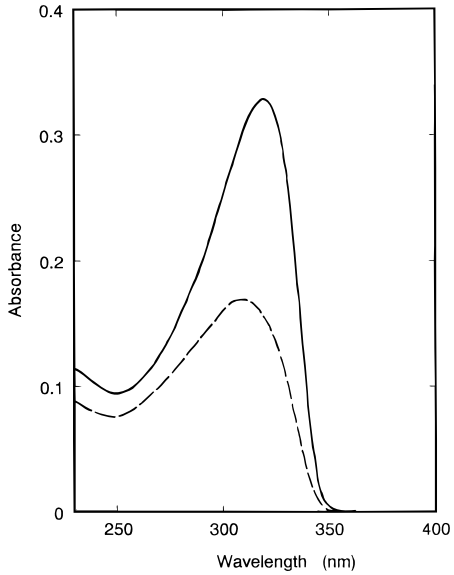

Figure 2. Polarized UV spectra of PMOdS film stretched on PP at 140 °C (draw ratio: 11×): (—) parallel polarization; (– –) perpendicular polarization.

intense reflection (d = 0.410 nm) and several small peaks (d = 1.415, 0.909, 0.783, and 0.665 nm) are observed in the range $2\theta = 5-25°$. These reflections are however broad and overlap with each other, suggesting a low degree of periodic order in the crystal lattice.[37]

The solution-cast film of PMOdS shows a thermochromic transition in the UV spectrum associated with the phase transition. A UV absorption peak is observed at 308 nm below 45 °C, and the peak shifts to 300 nm above 55 °C. Only a small shift of the UV peak suggests that the phase transition does not cause drastic changes in the main-chain conformation. The conformation of molecular chains is poorly ordered containing gauche Si−Si bonds even in the low-temperature phase.

Orientation Development in PMOdS Film Stretched on Supporting Polymer Substrates. The stretched PMOdS films were composed of two layers. The thin layer contacting the supporting film was oriented and was not soluble in hexane. A thick layer on it was however almost isotropic. The unoriented layer was extracted with hexane, and the remaining oriented layer was used for the spectroscopic measurements. Although PMOdS is known as one of the soluble polysilanes, the thin oriented layer of PMOdS barely dissolves in organic solvents. The decrease of absorbance of the UV spectrum is less than 10% even when the sample film is immersed in hexane at 40 °C for 150 h.

Figure 2 shows the polarized UV spectra of PMOdS stretched on PP. The transition moment of the lowest $\sigma-\sigma^*$ electronic transition of polysilanes is parallel to the silicon backbone. As the absorption intensity for the parallel polarization is higher than that for the perpendicular polarization, the silicon main chains are oriented parallel to the stretching direction. The absorption peak for the perpendicular polarization is observed at 307 nm similarly to that for the as-cast film, whereas the peak for the parallel polarization shifts to 322 nm. The drawing stress changes the backbone conformation of oriented molecular chains into the extended form with trans-rich segments. Figure 3 shows the polarized UV spectra of PMOdS stretched on PE. In contrast to the PMOdS film on PP, the main chains of PMOdS are oriented perpendicular to the draw direction on PE. The

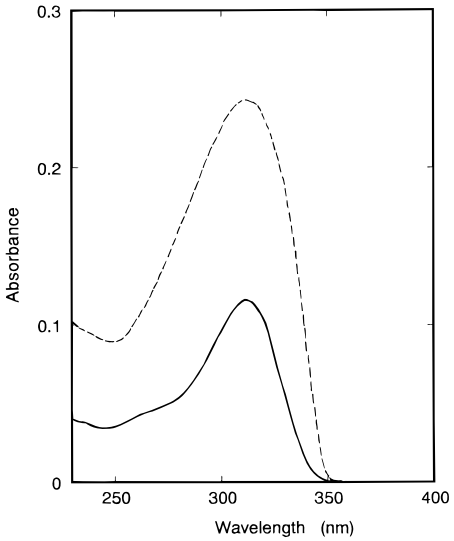

Figure 3. Polarized UV spectra of PMOdS film stretched on PE at 120 °C (draw ratio: 9.2×): (—) parallel polarization; (– –) perpendicular polarization.

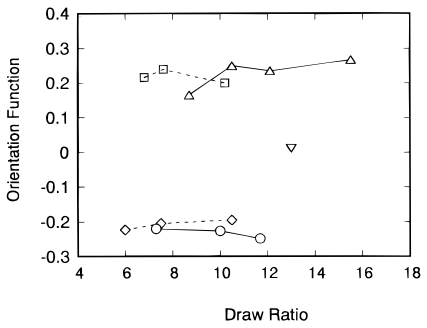

Figure 4. Orientation functions of stretched PMOdS as a function of draw ratio: (◇) PE, XX °C; (○) PE, 120 °C; (□) PP, 70 °C; (△) PP, 140 °C; (▽) PVA, 140 °C.

absorption maximum is observed around 313 nm for both polarizations.

Figure 4 summarizes the effects of draw ratio, drawing temperature, and substrate polymers on the orientation function. The orientation function, f, was calculated from the dichroic ratio, D.

$$f = (D - 1)/(D + 2) \qquad (1)$$

The orientation function is not significantly affected by the draw ratio, but is much more sensitive to the substrate polymer. It is difficult to prepare the oriented films by stretching PMOdS on PVA. The orientation function does not much depend on the drawing temperature, if the samples are drawn above the phase transition temperature of PMOdS. In the melt-drawing process, the mobile chains of PMOdS are supported by the substrate polymers and are co-oriented with the supporting polymers by stretching to the higher draw ratio. If the stretching were carried out also below the phase transition of PMOdS, the PMOdS layer easily fractured at low elongation.

The scanning electron micrographs of the surface of drawn samples are shown in Figure 5. A number of fine fibrils are uniaxially oriented in the stretched film of PP without PMOdS, whereas the fine striations of the fibrillar morphology become obscured on the surface of PMOdS layer stretched on PP (Figure 5a,b). PMOdS is grooved in the interfibrillar region of the fibrillar

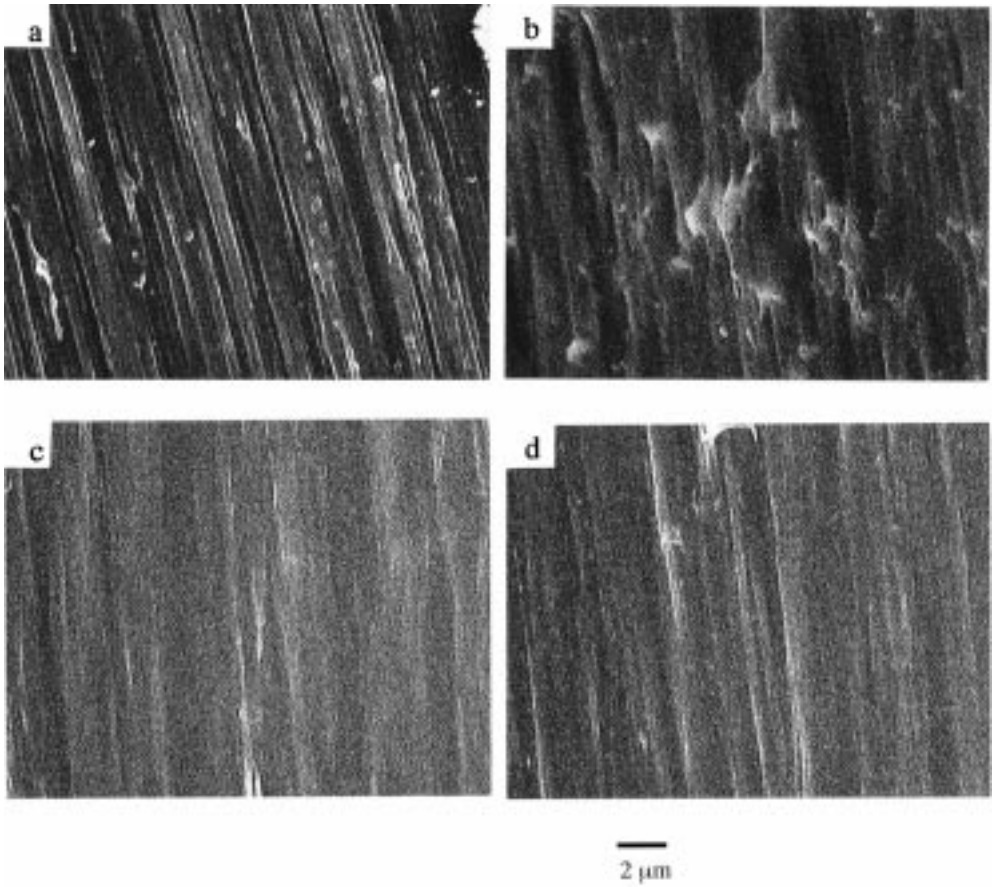

Figure 5. SEM photographs of drawn samples: (a) PP substrate without PMOdS (draw ratio: 11×); (b) PMOdS on PP substrate (draw ratio: 11×); (c) PE substrate without PMOdS (draw ratio: 9.2×); (d) PMOdS on PE substrate (draw ratio: 9.2×).

morphology of the stretched PP substrate and covers the surface of PP forming some lumpy structures. The height mode experiment of SFM shows that the mean surface roughness of PMOdS on PP is 450−500 nm around the lumpy structure and is larger than that for the bare surface of stretched PP (250 nm). In the regions without lumps, the mean surface roughness of PMOdS on PP is as small as 150 nm. The surface of the PE substrate was shown to be smoother (150−200 nm) than that for the PP substrate. The morphology of PMOdS on the PE substrate is similar to that of the bare surface of the drawn PE at this magnification (Figure 5c,d). As described before, the oriented PMOdS layer on the polymer substrates is not soluble in organic solvents, for which two possible causes can be considered. The polysilane domains are strongly adsorbed to the PE and PP substrates, or PMOdS is miscible with the substrate polymers and molecular chains so that the polysilane dissolves in the amorphous region of the substrate polymer. The latter is however improbable in the present case. Figure 6 shows the polarized optical micrograph of the PMOdS/PE blend. The morphology of the blend consists of the phase-separated domains of PE and PMOdS. In the case of PMOdS on the PP substrate, the smooth PMOdS layer is shown to cover the fibrillar surface of stretched PP. The oriented layer of PMOdS is firmly adsorbed to the polymer substrate, forming a thin surface layer whose solubility is restricted by the interfacial interaction with the substrate.

Figure 7 shows the magnified views of surface morphology observed by the friction mode experiment of SFM. Fibrillar structure is observed on the surfaces of the drawn PP and PE substrates without PMOdS.

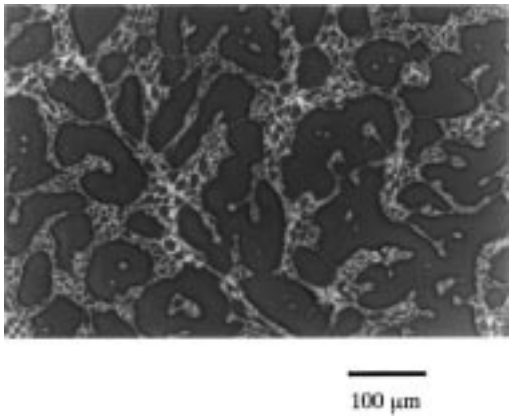

Figure 6. Polarized optical micrograph of PMOdS/PE (1:1) blend.

Diameters of stripes are 60−70 and 180−220 nm for PP and PE, respectively (Figure 7a,c). Closely packed domains of PMOdS are observed on the surface of the film stretched on the polymer substrates (Figure 7b,d). As the domains of PMOdS grow on the fibrillar morphology of the polymer substrate, the size and shape of the domains are affected by the morphology of the substrate. The domains of PMOdS grown on the fibrilar morphology of PP are elongated in the stretching direction, and the width of the domains matches with the fibril diameter of the PP substrate (Figure 7a,b). The molecular chains of PMOdS orient in the long axis of the domains. The domain size of PMOdS on the PE substrate is also similar to the fibril diameter of the PE substrate (Figure 7c,d), which is much larger than the

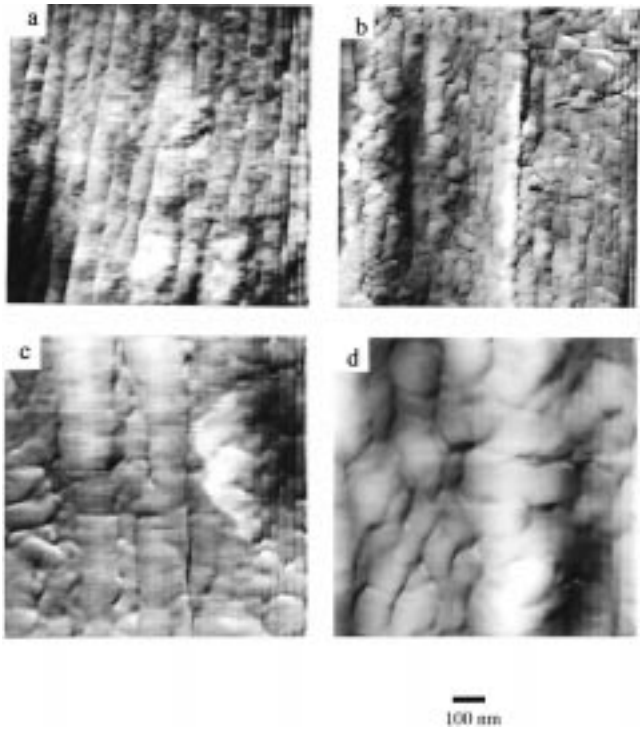

Figure 7. SFM images (friction mode) of drawn samples: (a) PP substrate without PMOdS (draw ratio: 11×); (b) PMOdS on PP substrate (draw ratio: 11×); (c) PE substrate without PMOdS (draw ratio: 9.2×); (d) PMOdS on PE substrate (draw ratio: 9.2×).

diameter of PP fibrils. Therefore, the domain size of PMOdS on PE is much larger than that of PMOdS on PP. The shape of the domains of PMOdS on PE is irregular and irrelevant to the orientation direction of the substrate polymer. The main chains of PMOdS are oriented in the perpendicular direction inside the domains of PMOdS on PE. Although the origin of the perpendicular orientation is not clearly known, one of the possible explanations is that the octadecyl chains orient along the molecular chains of polyethylene at the interface and that the orientation at the interface induces the oriented morphology of the whole domain.

In summary, the surface morphology of the polymer substrate affects the shape and size of the domains of PMOdS, which is closely related to the mode of molecular orientation of the PMOdS layer. Despotopoulou et al. discussed the effect of film thickness on the structural organization of spin-cast films of poly(di-*n*-hexylsilane).[32−35] This work demonstrates that the molecular orientation of the very thin films of polysilanes is affected by the surface morphology of the substrate polymers.

Orientation Development in PMOdS by Mechanical Deposition. The mechanically deposited films are smooth and uniform, when are observed with a polarizing optical microscope under crossed polarizations (Figure 8). Fine striations are observed to be running along the sliding direction, suggesting that the oriented morphology is formed by the mechanical deposition. Figure 9 shows the polarized UV spectra of the PMOdS films prepared by the mechanical deposition method. The molecular chains are oriented parallel to the stretching direction. The absorption maximum for the parallel polarization shifts to 320 nm, suggesting that the friction force is transmitted to the silicon main

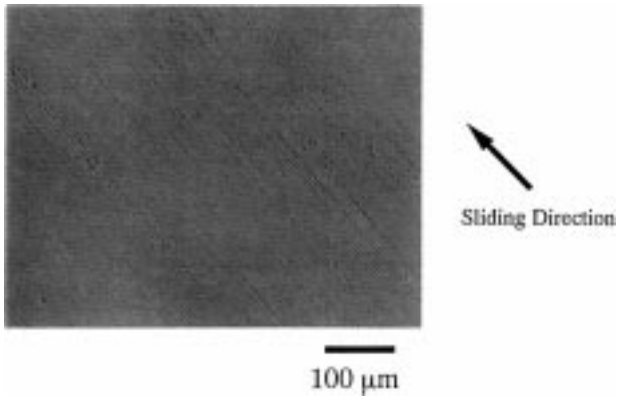

Figure 8. Polarized optical micrograph of PMOdS film mechanically deposited at 40 °C.

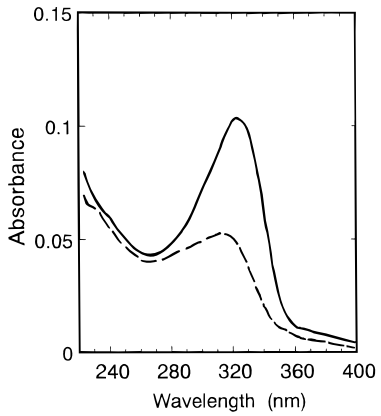

Figure 9. Polarized UV spectra of PMOdS film mechanically deposited at 40 °C: (—) parallel polarization; (– –) perpendicular polarization.

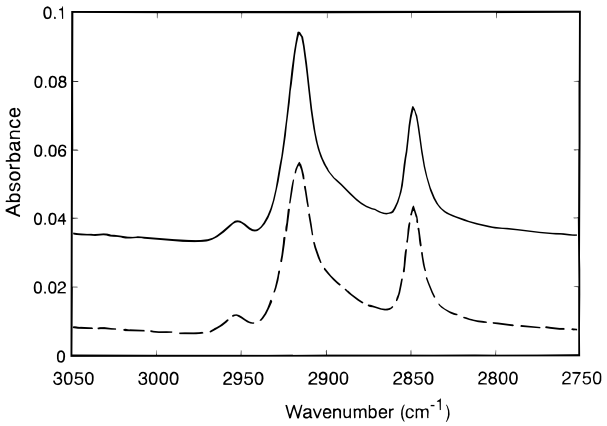

Figure 10. Polarized FTIR spectra of PMOdS film mechanically deposited at 40 °C: (—) parallel polarization; (– –) perpendicular polarization.

chains, and extends the molecular conformation of PMOdS.

Figure 10 shows the polarized FTIR spectra of mechanically deposited PMOdS. The absorption bands at 2848 and 2916 cm^{-1} are assigned to the symmetric and antisymmetric CH_2 stretching vibrations, respectively. The absorption intensity for the parallel polarization is slightly higher than that for the perpendicular polarization. Table 1 summarizes the orientation functions calculated from the polarized UV and IR spectra. The orientation function, f_{CH_2}, is defined as the degree of orientation of the axis normal to the HCH plane of the methylene units and represents the orientation function

Table 1. Orientation Functions of Main Chains and Side Chains of PMOdS

sample	f_{Si} (main chain)	f_{CH_2} (side chain)	$f_{CH_2antisym}$	f_{CH_2sym}
mechanical deposition film	0.210	−0.089	0.058	0.031
crystallized on PTFE	−0.112	0.416	−0.202	−0.214
crystallized on PDMS	−0.112			

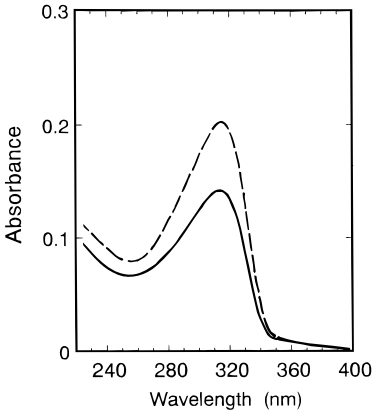

Figure 11. Polarized UV spectra of PMOdS film crystallized on the highly oriented PTFE film: (—) parallel polarization; (– –) perpendicular polarization.

of octadecyl chains, and f_{Si} stands for the orientation function of silicon main-chains, determined by the polarized UV spectra. The value of f_{CH_2} can be calculated from the orientation functions, f_{CH_2sym} and $f_{CH_2antisym}$, associated with the CH_2 symmetric and antisymmetric stretching vibrations, respectively, because the transition moments of these vibrations are normal to the octadecyl chains and perpendicular to each other. As the orientation functions of the three orthogonal axes sum up to zero,[37] f_{CH_2} is related to $f_{CH_2antisym}$ and f_{CH_2sym}.

$$f_{CH_2} = -f_{CH_2antisym} - f_{CH_2sym} \quad (2)$$

The Si main chains are oriented parallel to the sliding direction of the mechanical-deposition film, whereas the octadecyl chains are poorly oriented perpendicular to the sliding direction. The friction force orients the silicon backbone in the sliding direction, but is not effective on orienting the octadecyl chains. The low degree of perpendicular orientation in the octadecyl chains is induced by the parallel orientation of the Si main-chains.

Orientation Development in PMOdS by Crystallization on Highly Oriented PDMS and PTFE Substrates. Figures 11 and 12 show the polarized UV spectra of PMOdS films epitaxially crystallized on the highly oriented PTFE and PDMS films, respectively, which were prepared by the mechanical deposition method. PMOdS films were cast from hexane solution, in which PDMS and PTFE do not dissolve. A sharp absorption peak at 346 nm in Figure 12 is assigned to the lowest $\sigma-\sigma^*$ transition of PDMS. The orientation direction of the backbone of PMOdS is shown to be perpendicular to the orientation direction of molecular chains of PDMS and PTFE films. The degree of orientation of PMOdS on PDMS is similar to that for PMOdS on PTFE, suggesting that the substrate polymers have only minor effects on the orientation behavior. The degree of orientation decreases with increasing thickness of PMOdS films. For example, the orientation

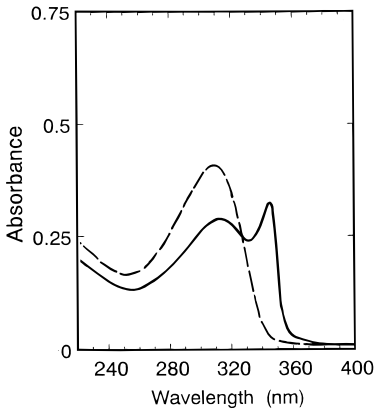

Figure 12. Polarized UV spectra of PMOdS film crystallized on the highly oriented PDMS film: (—) parallel polarization; (– –) perpendicular polarization.

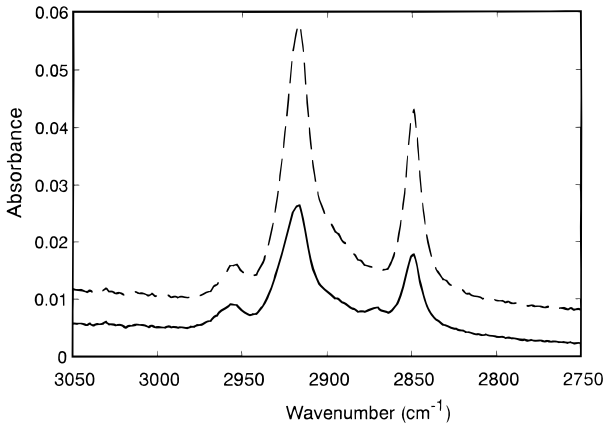

Figure 13. Polarized FTIR spectra of PMOdS film crystallized on the highly oriented PTFE film: (—) parallel polarization; (– –) perpendicular polarization.

function of PMOdS on PTFE changes from −0.145 to −0.040 with increasing thickness from 150 to 590 nm. The oriented structure of PDMS and PTFE is effective only on orienting a very thin layer near the interface.

Figure 13 shows the polarized FTIR spectra of PMOdS films crystallized on a highly oriented PTFE film. The absorbance for the perpendicular polarization is much higher than that for the parallel polarization in the range of CH_2 stretching vibrations. As the transition moments of CH_2 stretching vibrations are perpendicular to the octadecyl chains, the large perpendicular dichroism of the FTIR spectra shows that the octadecyl chains are highly oriented in the sliding direction. The orientation functions are shown in Table 1. The values of f_{CH_2} and f_{Si} suggest that the degree of orientation of octadecyl chains is higher than that of Si main chains and, thereby, that the dominant factor in the structural organization is the epitaxial orientation of the side chains along the oriented direction of the polymer substrate. It is interpreted that the oriented PDMS and PTFE layers selectively align the octadecyl side chains of PMOdS along their orientation directions and that the parallel orientation of octadecyl chains forces the silicon main chains to align perpendicular to the sliding direction. Analogous orientation behavior has been reported for poly(2,5-diheptyl-*p*-phenylene).[25]

Polarized Fluorescence Spectra. Figure 14 shows the polarized fluorescence spectra of drawn PMOdS on PP. The molecular chains are oriented along the draw direction in this sample. The fluorescence spectra show

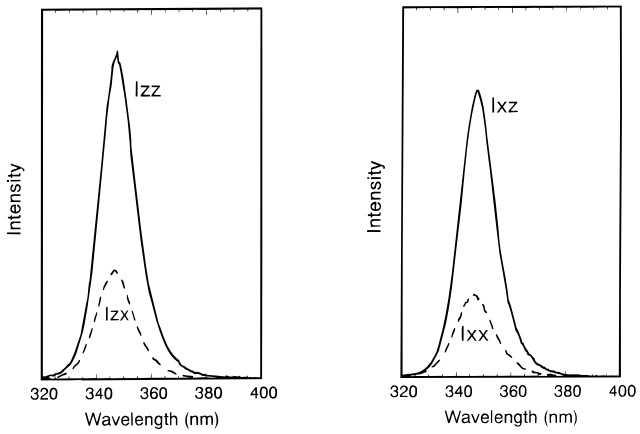

Figure 14. Polarized fluorescence spectra of PMOdS film stretched on PP at 140 °C (draw ratio: 11). The four spectra are drawn in the same scale.

an emission peak at 350 nm, and the peak position does not significantly shift by the excitation wavelength. If the transition moment angle does not change during the excitation−emission process, fluorescence intensity I_{xz} should agree with I_{zx}. The observed intensity, I_{xz} is however much higher than I_{zx}, indicating that the transition moment angle for the emission is different from the angle for the excitation. The orientation functions for the excitation site and for the emission site are treated independently in this work. The angles θ_{ex} and θ_{em} represent the angle between DD and the transition moment for the excitation and emission processes, respectively. The orientation functions, f_{ex} and f_{em}, for the excitation and emission sites, respectively, are defined by

$$f_{ex} = (3\langle\cos^2\theta_{ex}\rangle - 1)/2 \tag{3}$$

$$f_{em} = (3\langle\cos^2\theta_{em}\rangle - 1)/2 \tag{4}$$

where the $\langle\ \rangle$ averages over the spatial distribution of the transition moments. On the other hand, the fluorescence intensity of the polarized fluorescence is given by

$$I_{zz} = C\langle(\boldsymbol{M}_{ex}\cdot\boldsymbol{k})^2\rangle \times \langle(\boldsymbol{M}_{em}\cdot\boldsymbol{k})^2\rangle = C\langle\cos^2\theta_{ex}\rangle \times \langle\cos^2\theta_{em}\rangle \tag{5}$$

$$I_{zx} = C\langle(\boldsymbol{M}_{ex}\cdot\boldsymbol{k})^2\rangle \times \langle(\boldsymbol{M}_{em}\cdot\boldsymbol{i})^2\rangle = C\langle\cos^2\theta_{ex}\rangle \times \langle\sin^2\theta_{em}\rangle/2 \tag{6}$$

$$I_{xz} = C\langle(\boldsymbol{M}_{ex}\cdot\boldsymbol{i})^2\rangle \times \langle(\boldsymbol{M}_{em}\cdot\boldsymbol{k})^2\rangle = C\langle\sin^2\theta_{ex}\rangle \times \langle\cos^2\theta_{em}\rangle/2 \tag{7}$$

$$I_{xx} = C\langle(\boldsymbol{M}_{ex}\cdot\boldsymbol{i})^2\rangle \times \langle(\boldsymbol{M}_{em}\cdot\boldsymbol{i})^2\rangle = C\langle\sin^2\theta_{ex}\rangle \times \langle\sin^2\theta_{em}\rangle/4 \tag{8}$$

where $\boldsymbol{M}_{ex}$ and $\boldsymbol{M}_{em}$ stand for the unit vectors along the transition moment vectors for the excitation and emission, respectively, $\boldsymbol{i}$ and $\boldsymbol{k}$ are the unit vectors along the *X*- and *Z*-axes, respectively, and *C* is the proportional constant. The orientation functions can be calculated from the fluorescence intensities

$$\langle\cos^2\theta_{ex}\rangle = (I_{zz} + 2I_{zx})/C \tag{9}$$

$$\langle\cos^2\theta_{em}\rangle = (I_{zz} + 2I_{xz})/C \tag{10}$$

where

$$C = I_{zz} + 2I_{zx} + 2I_{xz} + 4I_{xx} \tag{11}$$

The orientation functions are calculated to be $f_{ex} = 0.063$ and $f_{em} = 0.407$ for the stretched PMOdS films. The result shows that the degree of orientation of the emission site is much higher than that of the excitation site.

It was reported that the molecular chains in poly(di-*n*-hexylsilylene) were separated into a series of chromophores communicating by a rapid energy transfer.[38] When the short trans segments are excited at a shorter wavelength, the electronic energy is transferred to the long segments, resulting in emission from the long trans segment. The difference of orientation function between the excitation and emission sites is interpreted as a result of the energy transfer between segments of PMOdS molecular chains. PMOdS shows broad absorption bands in the wavelength region 280−350 nm. The molecular chains of PMOdS are expected to contain various segments with different conformations, which would contribute to the broad UV absorption band. The extended segments rich in trans give rise to the optical absorption in the longer wavenumber region of the absorption band, whereas the coiled forms with disordered conformation absorb UV light in the shorter wavelength side of the band. The extended segments are oriented more highly to the drawing direction than the coiled segments by stretching the film. In fact, the dichroic ratio of the absorption spectra is higher in the longer wavelength region within the absorption band. The excitation site contains poorly oriented segments with disordered conformation, from which the electronic energy is transferred to the highly oriented segments with trans-rich conformations. The emission occurs from the highly oriented trans-rich segments with the lowest electronic energy. This view is in agreement with the polarization characteristics and the large Stokes shift in the fluorescence spectrum.

Conclusions

The orientation behavior of poly(methyloctadecylsilane), a comblike polymer having long side chains, was studied with polarized UV absorption spectroscopy. The two modes of molecular orientation compete with each other. One is the orientation of silicon backbone to the mechanical direction, which is caused by the transmission of applied stress to the silicon main chains. The other is the orientation of side chains to the mechanical direction, which forces the main chains to orient perpendicular to the mechanical direction. The main-chain orientation is the principal process in the case of drawing PMOdS films on PP and mechanical deposition of PMOdS itself. On the other hand, the side-chain orientation dominates over the main-chain orientation in the PMOdS film stretched on PE. When PMOdS is crystallized on the oriented PDMS and PTFE films, the side chains tend to orient in the orientation direction of the substrate polymers.

The mode of orientation of PMOdS films stretched on the polymer substrates was discussed in relation to the surface morphology of the polymer substrate. On the

thin fibrillar structure of PP substrates, one can observe long rectangular domains of PMOdS, whose widths approximately fit to the fiber diameter of PP. On the other hand, the larger domains with isotropic dimensions are observed on the PE substrate, in which the fibrils are thicker than those in the PP substrates. The surface morphology of the polymer substrate affects the shape and size of the domains of PMOdS and thereby controls the orientation behavior of PMOdS.

The broad absorption band in the wavelength region of 280−350 nm consists of absorption bands with different peak positions. The segments with different conformations give rise to light absorption at each wavelength. The extended segments rich in trans conformation absorb UV light at longer wavelength than the coiled form with disordered conformation. The results of the polarized fluorescence confirm that the extended segments are more highly oriented than the coiled form, and that the electronic energy transfer occurs from the latter to the former during the excitation−emission process.

References and Notes

(1) Miller, R. D.; Michl, J. *Chem. Rev.* **1989**, *89*, 1359.
(2) Chen, D.; Hu, H. Macomol. *Chem. Phys.* **1994**, *195*, 2981.
(3) Kishida, H.; Tachibana, H.; Matsumoto, M.; Tokura, Y. *J. Appl. Phys.* **1995**, *78*, 3362.
(4) Suzuki, H. *Adv. Mater.* **1996**, *8*, 657.
(5) Abkowitz, M. A.; Stolka, M. *Synth. Met.* **1996**, *78*, 333.
(6) Ebihara, K.; Koshihara, S.; Miyazawa, T.; Kira, M. *Jpn. J. Appl. Phys.* **1996**, *35*, L1278
(7) Kyotani, H.; Tanigaki, N.; Minami, N. *Polym. Prepr. Jpn.* **1995**, *44*, 1543.
(8) van der Laan, G. P.; de Haas, M. P.; Hummel, A.; Frey, H.; Sheiko, S.; Möller, M. *Macromolecules* **1994**, *27*, 1897.
(9) Möller, M.; Frey, H.; Sheiko, S. *Colloid Polym. Sci.* **1993**, *271*, 554.
(10) Lovinger, A. J.; Davis, D. D.; Schilling, F. C.; Padden, F. J., Jr.; Bovey, F. A.; Zeigler, J. M. *Macromolecules* **1991**, *24*, 132.
(11) Embs, F. W.; Wegner, G.; Neher, D.; Albouy, P.; Miller, R. D.; Wilson, C. G.; Schrepp, W. *Macromolecules* **1991**, *24*, 5068.
(12) Seki, T.; Tamaki, T.; Ueno, K. *Macromolecules* **1992**, *25*, 3825.
(13) Kani, R.; Yoshida, H.; Nakano, Y.; Murai, S.; Mori, Y.; Kawata, Y.; Hayase, S. *Langmuir* **1993**, *9*, 3045.
(14) Yoshida, M.; Nakanishi, F.; Seki, T.; Sakamoto, K.; Sakurai, H. *Macromolecules* **1997**, *30*, 1860.
(15) Shimomura, M.; Ueno, K.; Okumoto, H.; Shen, J.; Itoh, K. *Macromolecules* **1994**, *27*, 7006.
(16) Takeuchi, K.; Mizoguchi, M.; Kira, M.; Shimana, M.; Furukawa, S.; Tamura, M. *J. Phys.: Condens. Matter* **1994**, *6*, 10705.
(17) Yatabe, T.; Shimomura, M.; Kaito, A. *Chem. Lett.* **1996**, 551.
(18) Pooley, C. M.; Tabor, D. *Proc. R. Soc. London, A* **1972**, *329*, 251.
(19) Wittmann, J. C.; Smith, P. *Nature* **1991**, *352*, 414.
(20) Fenwick, D.; Ihn, K. J.; Motamedi, F.; Wittmann, J. C.; Smith, P. *J. Appl. Polym. Sci.* **1993**, *50*, 1151.
(21) Dietz, P.; Hansma, P. K.; Ihn, K. J.; Motamedi, F.; Smith, P. *J. Mater. Sci.* **1993**, *28*, 1372.
(22) Tanigaki, N.; Yase, K.; Kaito, A.; Ueno, K. *Polymer* **1995**, *36*, 2477.
(23) Tanigaki, N.; Yase, K.; Kaito, A. *Thin Solid Films* **1996**, *273*, 263.
(24) Tanigaki, N.; Kyotani, H.; Wada, M.; Kaito, A.; Yoshida, Y.; Han, E.-M.; Abe, K.; Yase, K. *Thin Solid Films* **1998**, *331*, 229.
(25) Fahlman, M.; Rasmusson, J.; Kaeriyama, K.; Clark, D. T.; Beamson, G.; Salaneck, W. R. *Synth. Met.* **1994**, *66*, 123.
(26) Damman, P.; Dosiere, M.; Smith, P.; Wittmann, J. C. *J. Am. Chem. Soc.* **1995**, *117*, 1117.
(27) Tanigaki, N.; Yase, K.; Kaito, A. *Mol. Cryst. Liq. Cryst.* **1995**, *267*, 335.
(28) Frey, H.; Sheiko, S.; Möller, M.; Wittmann, J. C. *Adv. Mater.* **1993**, *5*, 917.
(29) Sheiko, S.; Blommers. B.; Frey, H.; Möller, M. *Langmuir* **1996**, *12*, 584.
(30) Frey, H.; Möller, M.; Turetskii, A.; Lotz, B.; Matyjaszewski, K. *Macromolecules* **1995**, *28*, 5498.
(31) Tanigaki, N.; Yoshida, Y.; Yase, K.; Kaito, A.; Kyotani, H. *Mol. Cryst. Liq. Cryst.* **1997**, *294*, 39.
(32) Despotopoulou, M. M.; Frank, C. W.; Miller, R. D.; Rabolt, J. F. *Macromolecules* **1995**, *28*, 6687.
(33) Frank, C. W.; Rao, V.; Despotopoulou, M. M.; Pease, R. F. W.; Hingsberg, W. D.; Miller, R. D.; Rabolt, J. F. *Science* **1996**, *273*, 912.
(34) Despotopoulou, M. M.; Miller, R. D.; Rabolt, J. F.; Frank, C. W. *J. Polym. Sci., Polym. Phys.* **1996**, *34*, 2335.
(35) Despotopoulou, M. M.; Frank, C. W.; Miller, R. D.; Rabolt, J. F. *Macromolecules* **1996**, *29*, 5797.
(36) Kaito, A.; Nakayama, K. *J. Polym. Sci, Polym. Phys.* **1994**, *32*, 691.
(37) Stein, R. S. *J. Polym. Sci.* **1958**, *31*, 327.
(38) Kligensmith, K. A.; Downing, J. W.; Miller, R. D.; Michl, J. *J. Am. Chem. Soc.* **1986**, *108*, 7438.

MA980390Y